

INVERSE GEOMETRY PROBLEM OF ESTIMATING THE LOCATION OF THE 1150°C ISOTHERM IN A BLAST FURNACE HEARTH

Marcial Gonzalez and Marcela B. Goldschmit

Centro de Investigación Industrial, FUDETEC

Dr. Simini 250, 2804 Campana, Argentina

e-mail: sidmgo@siderca.com

Key Words: Inverse geometry problem, Gauss Newton iterative regularization method, Blast furnace.

Abstract. *The hearth life is the key factor for the campaign length of a blast furnace and, in order to understand the wear mechanisms, it's useful to be able to estimate the location of the 1150°C isotherm because it represents a potential limit on the penetration of the liquid iron into the hearth wall.*

The location of the 1150°C isotherm can be estimated solving a nonlinear inverse heat transfer problem, based on the thermocouples located inside the hearth. As the domain of the heat transfer problem is unknown, a set of parameters is defined in order to describe it. These parameters are the inverse geometry heat transfer problem unknowns. In previous publications (M. Gonzalez et al., 4th IAS Ironmaking Conference, Nov. 2003, 381-386) the authors have presented this inverse geometry model applied to a unidimensional geometry.

In this work we reformulate the model for a bidimensional geometry, where the iteratively regularized Gauss-Newton method is used to solve the nonlinear inverse problem, Radial Basis Functions (RBF) are used to describe the geometry from a set of parameters, and remeshing techniques are used to discretize the domain. We describe the developed bidimensional inverse model and validate the solution against simulated measurements with different levels of noise.

1 INTRODUCTION

One of the most critical parts of the blast furnace is its hearth, which cannot be repaired or relined without interrupting its production for a long. Therefore, the blast furnace campaign is mainly limited by the hearth refractory wear produced by thermo-chemical solution and thermo-mechanical damage¹. Unfortunately, it is not possible to do direct measurements of the remaining lining thickness, so the thermal state of the blast furnace hearth is valuable information to estimate the erosion profile. In particular, it is useful to be able to estimate the location of the 1150°C isotherm because it represents a potential limit on the penetration of liquid iron into the hearth wall porosity (1150°C is the eutectic temperature of carbon saturated iron¹).

The location of the 1150°C isotherm can be estimated solving a nonlinear inverse heat transfer problem based on the thermocouples located inside the hearth²⁻⁵. The purpose of inverse heat transfer problems is to recover causal characteristics from information about the temperature field, while the purpose of direct problems is to specify the cause and effect relationships. Causal characteristics of heat transfer are boundary conditions and their parameters, initial conditions, thermophysical properties, as well as geometric characteristics of the studied object. Our general problem is an *inverse geometry heat transfer problem* where the observations are temperature measurements at points inside the object and the unknown is the geometry of the volume where the problem is defined. In Section 2, we formally define the general problem and describe the finite element model developed for the direct heat transfer problem.

It is well known that inverse problems are typically ill-posed in the sense that small observation perturbations can lead to big errors in the solution, so regularization methods have to be applied in order to guarantee a stable solution. Several regularization methods have been used in the literature to handle nonlinear ill-posed problems^{6,7}. Iterative regularization appears to be one of the most efficient approaches for the construction of stable algorithms for solving nonlinear inverse problems⁷ and, among them, we use the iteratively regularized Gauss-Newton method⁸⁻¹¹. In Section 3, we formulate the inverse geometry problem, considering the case of a linear combination of several regularization matrices.

The geometry is described by Radial Basis Functions (RBF) from a set of interpolation points, and these interpolation points are defined by a set of parameters which are actually the inverse geometry problem unknowns. We use Radial Basis Functions because they impose few restrictions on the geometry of the interpolation points which do not need to lie on a regular grid and provide a smooth interpolation¹²⁻¹⁵. In Section 4, we present the parametrization of the geometry and introduce Radial Basis Functions.

Finally, in Section 5, we develop the industrial application of estimating the location of the 1150°C isotherm in a blast furnace hearth. We also validate the solution of the algorithm against simulated measurements with different levels of noise and study its behavior on different regularization matrices.

2 DEFINITION OF THE GENERAL PROBLEM

Consider a general steady-state heat transfer problem defined on an arbitrary volume (Ω) which has a fixed boundary ($\partial\Omega_n$) where natural boundary conditions are applied, and an unknown boundary ($\partial\Omega_T$) where a known temperature is applied. As the volume Ω has different materials located on fixed positions, it will contain only some of them depending on the location of the boundary $\partial\Omega_T$ (Fig. 1).

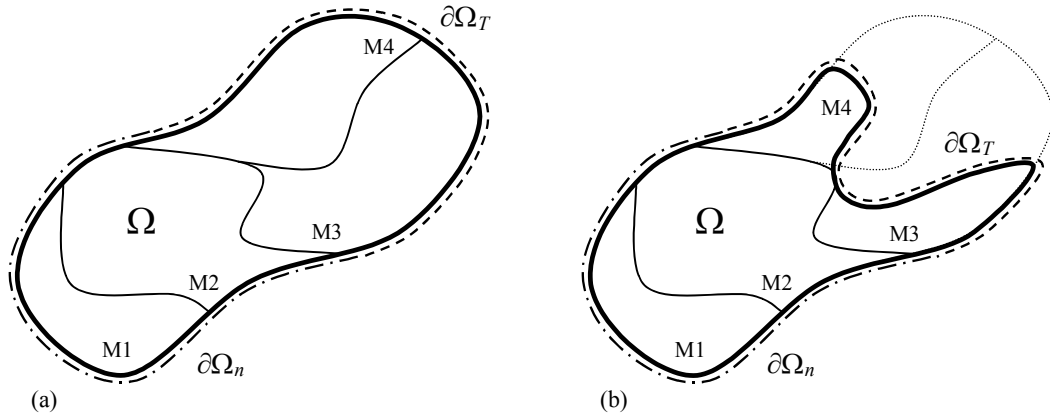


Figure 1: Schematic of the general problem.

Our aim is to determine the location of the boundary $\partial\Omega_T$, and so the geometry of the volume Ω , matching a set of temperatures measured at certain points located inside the volume. Therefore, our general problem is an inverse geometry heat transfer problem where the observations are temperature measurements at points inside the volume and the unknown is the geometry of the volume where the problem is defined.

2.1 The direct heat transfer problem

The solution of any inverse problem requires the solution of a direct problem. Our direct problem is a steady-state heat transfer problem governed by

$$\nabla \cdot (k \nabla T) = 0 \quad \forall \mathbf{x} \in \Omega, \quad (1)$$

where k is the temperature-dependant thermal conductivity, $\Omega \subset \mathbb{R}^{n_{\text{dim}}}$ is a bounded domain with $1 \leq n_{\text{dim}} \leq 3$, and $\partial\Omega$ is the smooth boundary of Ω .

Eq. (1) is subjected to the following boundary conditions on $\partial\Omega_T$, $\partial\Omega_q$ and $\partial\Omega_c$, complementary parts of $\partial\Omega$ ($\partial\Omega_n = \partial\Omega_q \cup \partial\Omega_c$, $\partial\Omega_q \cap \partial\Omega_c = \emptyset$ and $\partial\Omega = \partial\Omega_T \cup \partial\Omega_n$, $\partial\Omega_T \cap \partial\Omega_n = \emptyset$):

- Dirichlet boundary condition on $\partial\Omega_T$:

$$T = T_w \quad \forall \mathbf{x} \in \partial\Omega_T, \quad (2)$$

where T_w is a given imposed temperature.

- Neumann boundary condition on $\partial\Omega_q$:

$$-k \nabla T \cdot \mathbf{n} = q_w \quad \forall \mathbf{x} \in \partial\Omega_q, \quad (3)$$

where q_w is a given normal heat flux and \mathbf{n} is the outward normal to the surface $\partial\Omega$.

- Robin boundary condition on $\partial\Omega_c$:

$$-k \nabla T \cdot \mathbf{n} = h (T - T_\infty) \quad \forall \mathbf{x} \in \partial\Omega_c, \quad (4)$$

where h is the convective heat transfer coefficient and T_∞ is the ambient temperature.

The direct problem is solved using the Galerkin finite element method^{16,17} with the following resulting system of equations

$$(\mathbf{K}^k + \mathbf{K}^c) \mathbf{T}^{FEM} - \mathbf{F} = \mathbf{0}, \quad (5)$$

where \mathbf{T}^{FEM} is the vector of nodal temperatures, \mathbf{K}^k is the conductivity matrix, \mathbf{K}^c is the thermal convection matrix and \mathbf{F} is the thermal load vector, given by

$$\tilde{T} = \mathbf{N} \mathbf{T}^{FEM}, \quad (6)$$

$$\mathbf{K}^k = \int_{\Omega} \mathbf{B}^T \mathbf{k} \mathbf{B} dV, \quad (7)$$

$$\mathbf{K}^c = \int_{\partial\Omega_c} h \mathbf{N}^T \mathbf{N} dS, \quad (8)$$

$$\mathbf{F} = \int_{\partial\Omega_c} h \mathbf{N}^T T_\infty dS - \int_{\partial\Omega_q} \mathbf{N}^T q_w dS, \quad (9)$$

where \tilde{T} is the approximated temperature field, \mathbf{N} is the finite element interpolation matrix, and \mathbf{B} is the temperature-gradient interpolation matrix whose components are $B_{ij} = \frac{\partial N_j}{\partial x_i}$.

The equations are nonlinear because the thermal conductivity is temperature-dependant; therefore, it is necessary to solve them using an iterative technique.

3 FORMULATION OF THE INVERSE GEOMETRY PROBLEM

Since we are interested in practical applications, we have to consider our problem in finite-dimensional subspaces. This means that not only the number of measurements is finite, but also the location of the unknown boundary $\partial\Omega_T$ is parametrized in order to obtain the approximate solution numerically.

Therefore, we parametrize the location of the unknown boundary $\partial\Omega_T$ by a set of n_p parameters $\mathbf{p} = (p_1, \dots, p_{n_p})$, and we pose the inverse problem as finding the geometry parameters \mathbf{p}^* such that

$$\mathbf{p}^* = \arg \min_{\mathbf{p} \in \mathbb{R}^{n_p}} \mathcal{F}(\mathbf{p}) \quad (10)$$

where $\mathcal{F}_{(\mathbf{p})}$ is a function defined by the least-square error between the calculated and measured temperatures, given by

$$\mathcal{F}_{(\mathbf{p})} = \frac{1}{2} \left\| \mathbf{T}_{(\mathbf{p})} - \mathbf{T}^{OBS} \right\|^2 = \frac{1}{2} \sum_{i=1}^{n_{obs}} \left[\tilde{T}_{(\mathbf{x}_i^{OBS}, \mathbf{p})} - T_i^{OBS} \right]^2, \quad (11)$$

where T_i^{OBS} is the temperature measured at point \mathbf{x}_i^{OBS} , $\tilde{T}_{(\mathbf{x}_i^{OBS}, \mathbf{p})}$ is the temperature calculated by the finite element model using the geometry parameters \mathbf{p} , and n_{obs} is the number of observations.

It is well known that inverse problems are typically ill-posed in the sense that small observation perturbations can lead to big errors in the solution, so regularization methods have to be applied in order to guarantee a stable solution. Several regularization methods have been used in the literature to handle nonlinear ill-posed problems^{6,7} and, among them, iterative regularization appears to be one of the most efficient approaches for the construction of stable algorithms⁷.

3.1 Iteratively regularized Gauss-Newton method

We use a discrete scheme of the iteratively regularized Gauss-Newton method⁸⁻¹¹, whose iterative solution is defined by:

$$\begin{aligned} {}^{GN} \mathbf{p}^{Iter+1} = \mathbf{p}^{Iter} + & \left[\mathbf{DT}_{(\mathbf{p}^{Iter})}^T \mathbf{DT}_{(\mathbf{p}^{Iter})} + \alpha_{Iter} \mathbf{L}^T \mathbf{L} \right]^{-1} \\ & \cdot \left[\mathbf{DT}_{(\mathbf{p}^{Iter})}^T \Delta \mathbf{T}_{(\mathbf{p}^{Iter})}^{OBS} + \alpha_{Iter} \mathbf{L}^T \mathbf{L} (\mathbf{p}^\Delta - \mathbf{p}^{Iter}) \right] \end{aligned} \quad (12)$$

where $Iter$ denotes the iteration number; $\mathbf{DT}_{(\mathbf{p})}$ is the sensitivity matrix; \mathbf{L} is some regularization matrix; $\Delta \mathbf{T}_{(\mathbf{p})}^{OBS}$ is a vector whose components are $\left[T_i^{OBS} - \tilde{T}_{(\mathbf{x}_i^{OBS}, \mathbf{p})} \right]$ with $i = 1, n_{obs}$; \mathbf{p}^Δ is a priori suitable approximation of the unknown set of parameters; and $\alpha_{Iter} > 0$ is the regularization parameter.

The solution calculated with the iteratively regularized Gauss-Newton method, ${}^{GN} \mathbf{p}^{Iter+1}$, is used to update \mathbf{p}^{Iter} as follows

$$\mathbf{p}^{Iter+1} = \mathbf{p}^{Iter} + \beta^{Iter} \left({}^{GN} \mathbf{p}^{Iter+1} - \mathbf{p}^{Iter} \right) \quad (13)$$

where $\beta^{Iter} > 0$ is a step length such that

$$\mathcal{F}_{(\mathbf{p}^{Iter+1})}^* < \mathcal{F}_{(\mathbf{p}^{Iter})}^*, \quad (14)$$

with

$$\mathcal{F}_{(\mathbf{p})}^* = \frac{1}{2} \left\| \mathbf{T}_{(\mathbf{p})} - \mathbf{T}^{OBS} \right\|^2 + \frac{1}{2} \alpha \left\| \mathbf{L} (\mathbf{p} - \mathbf{p}^\Delta) \right\|^2. \quad (15)$$

The selection of a step length makes sense due to the highly non-linear nature of the function $\mathcal{F}_{(\mathbf{p})}^*$, in which case β^{Iter} is typically less than 1.00.

The iterative process is repeated until the following convergence criterion is satisfied

$$\frac{\left\| \mathbf{T}_{(\mathbf{p}^{Iter+1})} - \mathbf{T}_{(\mathbf{p}^{Iter})} \right\|}{\left\| \mathbf{T}_{(\mathbf{p}^{Iter})} \right\|} \leq TOL \cdot \beta^{Iter}. \quad (16)$$

3.1.1 Evaluation of the sensitivity matrix

The components of the sensitivity matrix are the partial derivatives of the temperature with respect to the set of geometry parameters. We evaluate them using a “discretize-then-differentiate” approach¹⁸, which means that we first discretize the temperature field and then we differentiate it. So, we apply a finite difference approximation of each partial derivative

$$\left. \frac{\partial T}{\partial p_j} \right|_{(\mathbf{x}, \mathbf{p})} \approx \frac{\tilde{T}(\mathbf{x}, \{p_1, \dots, p_j + \Delta p_j, \dots, p_{n_p}\}) - \tilde{T}(\mathbf{x}, \{p_1, \dots, p_j, \dots, p_{n_p}\})}{\Delta p_j}. \quad (17)$$

Therefore, the sensitivity matrix can be written as

$$\mathbf{DT}_{(\mathbf{p})} = \begin{bmatrix} \mathbf{N}_{(\mathbf{x}_1^{OBS})} \left. \frac{\partial \mathbf{T}}{\partial p_1} \right|_{(\mathbf{p})}^{FEM} & \cdots & \mathbf{N}_{(\mathbf{x}_1^{OBS})} \left. \frac{\partial \mathbf{T}}{\partial p_{n_p}} \right|_{(\mathbf{p})}^{FEM} \\ \vdots & \ddots & \vdots \\ \mathbf{N}_{(\mathbf{x}_{n_{obs}}^{OBS})} \left. \frac{\partial \mathbf{T}}{\partial p_1} \right|_{(\mathbf{p})}^{FEM} & \cdots & \mathbf{N}_{(\mathbf{x}_{n_{obs}}^{OBS})} \left. \frac{\partial \mathbf{T}}{\partial p_{n_p}} \right|_{(\mathbf{p})}^{FEM} \end{bmatrix} \in \mathbb{R}^{n_{obs} \times n_p}, \quad (18)$$

where $\left. \frac{\partial \mathbf{T}}{\partial p_j} \right|_{(\mathbf{p})}^{FEM}$ are vectors of nodal sensitivities with respect to the parameter p_j , such that

$$\left. \frac{\partial T}{\partial p_j} \right|_{(\mathbf{x}, \mathbf{p})} \approx \mathbf{N}_{(\mathbf{x})} \left. \frac{\partial \mathbf{T}}{\partial p_j} \right|_{(\mathbf{p})}^{FEM}. \quad (19)$$

The components of these nodal sensitivity vectors can be easily obtained from definition (17) because the finite element discretization support is the same as the one we use for the temperature field.

3.1.2 Evaluation of the regularization matrix

The regularization matrix \mathbf{L} is the discrete form of some differential operator^{11,19}. We choose a combination of the identity matrix \mathbf{I} and discrete approximations of derivative operators given by

$$\mathbf{L}^T \mathbf{L} = \sum_{k=0}^2 w_k \mathbf{L}_k^T \mathbf{L}_k, \quad (20)$$

where

$$\mathbf{L}_0 = \mathbf{I} \in \mathbb{R}^{n_p \times n_p} \quad (21)$$

$$\mathbf{L}_1 = \begin{bmatrix} 1 & -1 & & \\ & \ddots & \ddots & \\ & & 1 & -1 \end{bmatrix} \in \mathbb{R}^{(n_p-1) \times n_p} \quad (22)$$

$$\mathbf{L}_2 = \begin{bmatrix} 1 & 2 & -1 & & \\ & \ddots & \ddots & \ddots & \\ & & 1 & 2 & -1 \end{bmatrix} \in \mathbb{R}^{(n_p-2) \times n_p} \quad (23)$$

and $w_k \geq 0$ are weighting factors such that $\sum_{k=0}^2 w_k = 1$. In Section 5, we study the solution behavior on different regularization matrices.

3.1.3 Determination of the regularization parameter

The regularization parameter $\alpha_{Iter} > 0$ is *a priori* chosen such that

$$1 \geq \frac{\alpha_{Iter+1}}{\alpha_{Iter}} \geq r, \quad \lim_{Iter \rightarrow \infty} \alpha_{Iter} = 0 \quad (24)$$

with $r < 1$. This monotonically decreasing sequence has as its first term the optimal regularization parameter for the Tikhonov regularization method⁶

$$\alpha_0 \sim \delta^{\frac{2}{2\nu+1}}, \quad \nu \in [1/2; 1] \quad (25)$$

where δ is called the noise level.

3.2 The algorithm

In Fig.2 we show the iterative algorithm of the nonlinear inverse problem. There are three different steps involved in the iterative process:

- the solution of the direct problem,
- the evaluation of the sensitivity matrix, which requires to solve the direct problem several times, and
- the determination of the iteratively regularized Gauss-Newton method solution, which also requires to solve the direct problem several times when the optimal step length is determined.

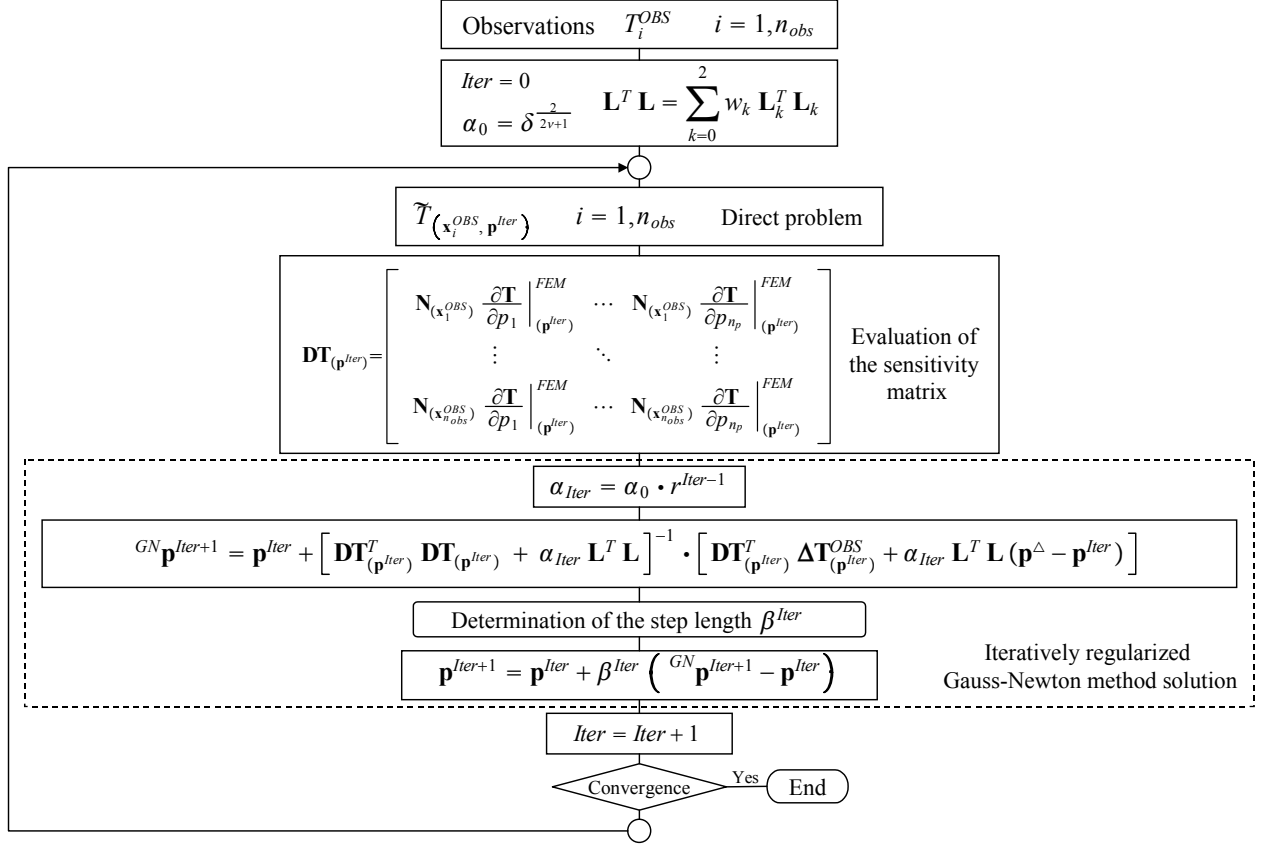


Figure 2: Iterative algorithm of the nonlinear inverse problem.

4 PARAMETRIZATION OF THE GEOMETRY

As stated in Section 3, the location of the unknown boundary $\partial\Omega_T$ is parametrized by a set of n_p parameters $\mathbf{p} = (p_1, \dots, p_{n_p})$. Each parameter p_i has a base point with coordinates \mathbf{BP}_{p_i} , and a direction vector \mathbf{DV}_{p_i} , such that a point on the unknown boundary is defined by

$$\mathbf{SP}_{p_i} = \mathbf{BP}_{p_i} + p_i \mathbf{DV}_{p_i}. \quad (26)$$

As an example, we show in Fig.3 a set of base points and direction vectors which are used to describe the location of the unknown boundary $\partial\Omega_T$, but clearly their location and orientation depend on the geometry of each problem.

Then, given a set of surface points, the location of the unknown boundary $\partial\Omega_T$ is approximated with a smooth function which interpolates them. For this purpose we use Radial Basis Functions because they impose few restrictions on the geometry of the interpolation points which do not need to lie on a regular grid, and provide a smooth interpolation^{12–15}. As a result, the domain where the direct heat transfer problem is stated is perfectly defined.

Finally, since the direct problem must be solved several times for each inverse problem iteration, changing the geometry parameters and so the domain to be discretized, we use remeshing

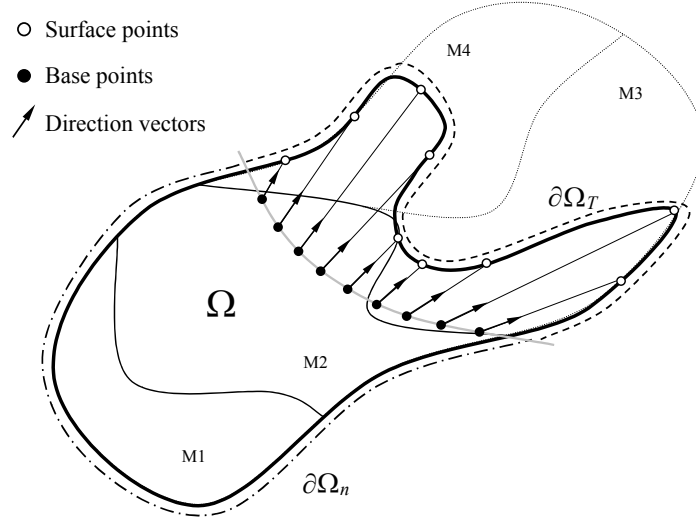


Figure 3: Schematic of the geometry parametrization.

techniques in order to solve it, for each given geometry.

4.1 Radial Basis Functions

The problem consists in finding an interpolation function $\Phi(\mathbf{x})$ given a set of n_{sp} points on the unknown boundary $\partial\Omega_T$ (where $\Phi = 0$) and a set of n_{ip} points inside the volume Ω (where $\Phi < 0$). For this purpose, we choose a Radial Basis Function defined by

$$\Phi(\mathbf{x}) = q(\mathbf{x}) + \sum_{i=1}^n \alpha_i R_{(\|\mathbf{x}-\mathbf{x}^i\|)} . \quad (27)$$

where $n = n_{sp} + n_{ip}$; $q(\mathbf{x})$ is a low degree polynomial; α_i are real numbers; and R is the basis function¹²⁻¹⁵.

In the specific case of thin plate spline functions on \mathbb{R}^2 , $R_{(r)}$ and $q(\mathbf{x})$ are defined as

$$R_{(r)} = r^2 \log(r) \quad (28)$$

$$q(\mathbf{x}) = q(x_1, x_2) = d_0 + d_1 x_1 + d_2 x_2 \quad (29)$$

and, as $\Phi(\mathbf{x})$ is chosen from the Beppo-Levi space of distributions on \mathbb{R}^2 with square integrable second derivative, some conditions must be imposed on α_i

$$\sum_{i=1}^n \alpha_i = \sum_{i=1}^n \alpha_i x_1^i = \sum_{i=1}^n \alpha_i x_2^i = 0 . \quad (30)$$

Therefore, the coefficients α_i and d_j are obtained from the following system of equations

$$\begin{bmatrix} \mathbf{A} & \mathbf{Q} \\ \mathbf{Q}^T & \mathbf{0} \end{bmatrix} \begin{pmatrix} \boldsymbol{\alpha} \\ \mathbf{d} \end{pmatrix} = \begin{pmatrix} \boldsymbol{\Phi} \\ \mathbf{0} \end{pmatrix} \quad (31)$$

where

$$A_{ij} = \|\mathbf{x}^i - \mathbf{x}^j\|^2 \log(\|\mathbf{x}^i - \mathbf{x}^j\|), \quad \mathbf{A} \in \mathbb{R}^{n \times n}; \quad (32)$$

$$\mathbf{Q} = \begin{bmatrix} 1 & x_1^1 & x_2^1 \\ \vdots & \vdots & \vdots \\ 1 & x_1^n & x_2^n \end{bmatrix} \in \mathbb{R}^{n \times 3}; \quad (33)$$

$$\boldsymbol{\alpha}^T = (\alpha_1 \quad \cdots \quad \alpha_n) \in \mathbb{R}^n; \quad (34)$$

$$\mathbf{d}^T = (d_0 \quad d_1 \quad d_2) \in \mathbb{R}^3; \quad (35)$$

$$\boldsymbol{\Phi}^T = (\Phi_{(\mathbf{x}^1)} \quad \cdots \quad \Phi_{(\mathbf{x}^n)}) \in \mathbb{R}^n. \quad (36)$$

Note that $\Phi_{(\mathbf{x}^i)}$ will be equal to zero except for the n_{ip} interior points.

5 INDUSTRIAL APPLICATION

In this section, we develop the industrial application of estimating the location of the 1150°C isotherm in a blast furnace hearth.

Regarding the direct problem, we model a vertical section of the lining (Fig. 4) with axisymmetric finite elements because the geometry of the blast furnace hearth is rotationally symmetric about an axis and is subjected to axisymmetric cooling conditions (Table 1). The hearth is built with refractories with different temperature-dependant thermal properties (Table 2), so we consider their dependence on the direct problem resolution, and their fixed location in the remeshing algorithm. The remeshing algorithm developed for this purpose is not discussed in this paper.

Regarding the inverse geometry problem, the number of observations (n_{obs}) is 28 because there are 28 thermocouples located inside the hearth (Fig. 4), and the number of parameters used to parametrize the location of the unknown boundary (n_p) is chosen to be 7. We show in Fig. 5 the set of base points and direction vectors which are used to describe the location of the 1150°C isotherm, where the set of surface points is interpolated using *thin plate spline* radial basis functions (see Section 4.1).

In order to validate the solution of the algorithm against measurement uncertainties, we simulate measurements with different levels of noise following these steps:

1. We define a “real geometry” described by a set of geometry parameters \mathbf{p}^{Real} .
2. We calculate the observations that correspond to the “real geometry”, \mathbf{T}^{Real} , assuming error free measurements.
3. We simulate measurements with different levels of noise ($noise = 5\%, 10\%, 15\%$) as follows

$$T_i^{OBS} = T_i^{Real} (1 + \xi \cdot noise) \quad (37)$$

where $\xi \in [-1; +1]$ is a uniformly distributed random disturbance.

Cooling zone	Convective cooling parameters	
Lower hearth spray	$h_{water} = 450 \text{ W/m}^2\text{°C}$	$T_{water} = 38\text{°C}$
Bottom cooling	$h_{air} = \left(120 - 90\frac{r}{r_{max}}\right) \text{ W/m}^2\text{°C}$	$T_{air} = \left(26 + 22\frac{r}{r_{max}}\right) \text{°C}$

Table 1: Cooling conditions.

Refractories	Thermal Conductivity	
SiC Castable	20.00 W/m K	
Mortar	1.00 W/m K	
Graphite EGF	130.00 W/m K	
Semi Graphite BC-30	31.67 W/m K	
Carbon BC-7S	T = 873 K	14.12 W/m K
	T = 1073 K	14.99 W/m K
	T = 1273 K	15.63 W/m K
	T = 1473 K	16.09 W/m K
SiC / Alumnina	7.20 W/m K	
High Fired Super Duty	T = 673 K	1.200 W/m K
	T = 973 K	1.300 W/m K
	T = 1373 K	1.500 W/m K
EG Ramming	T = 293 K	25.00 W/m K
	T = 473 K	20.00 W/m K
	T = 873 K	11.00 W/m K
	T = 1273 K	8.00 W/m K
	T = 1573 K	7.00 W/m K
Carbon BC-5	T = 873 K	16.96 W/m K
	T = 1073 K	17.66 W/m K
	T = 1273 K	18.13 W/m K
	T = 1473 K	18.36 W/m K

Table 2: Material Properties.

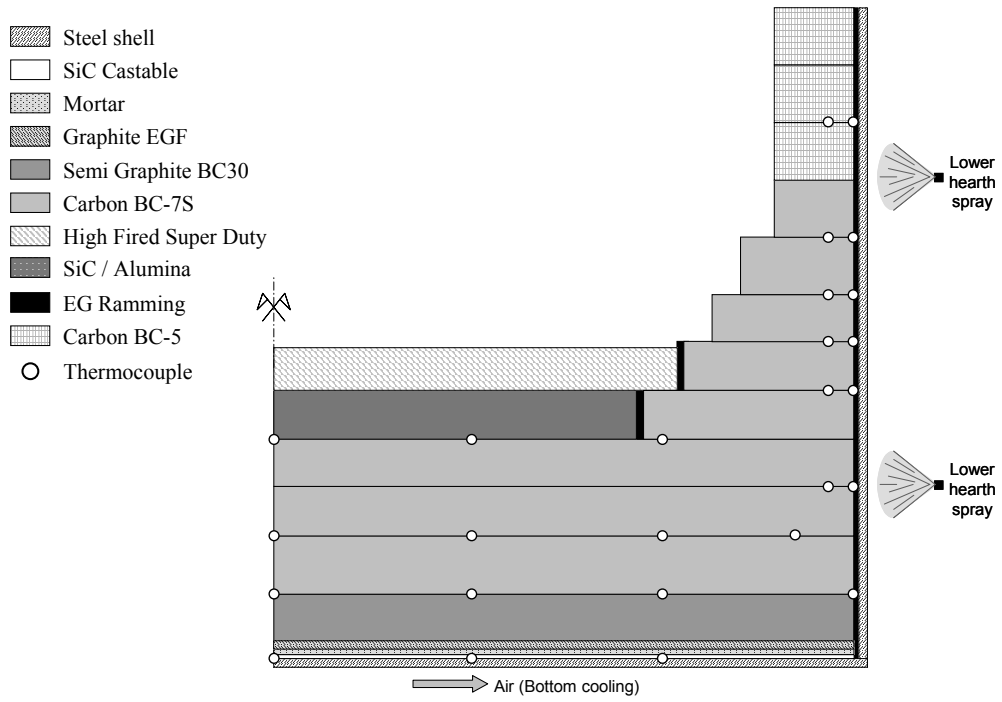


Figure 4: Vertical section of the blast furnace hearth.

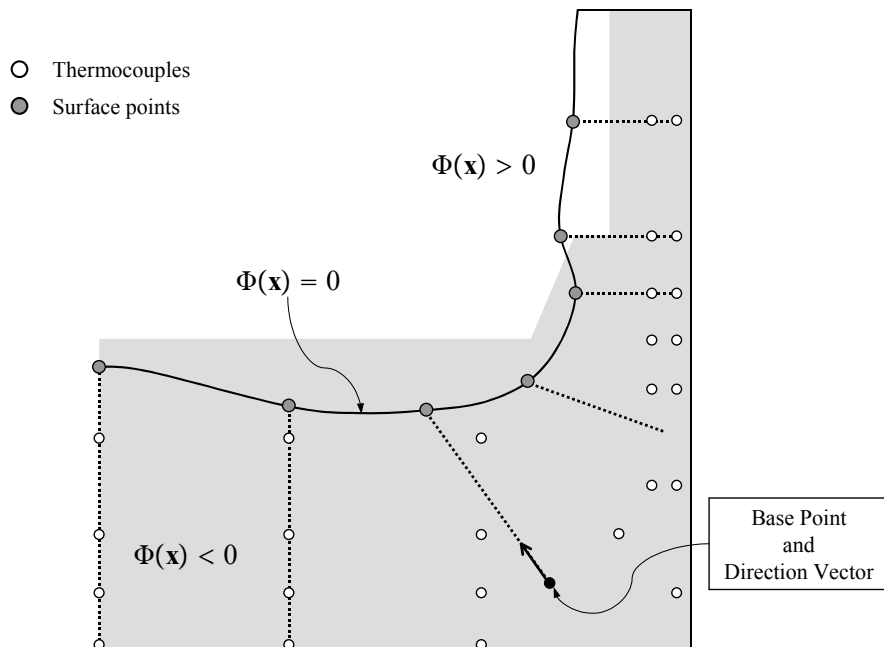


Figure 5: Parametrization of the unknown boundary location.

Then, we solve the inverse geometry problem for each set of observations, using as initial guess the regularization geometry $\mathbf{p}^0 = \mathbf{p}^\Delta$, and evaluate the following relative errors

$$\varepsilon_{obs} = \frac{\|\mathbf{T}_{(\mathbf{p}^{Iter})} - \mathbf{T}^{OBS}\|}{\|\mathbf{T}^{OBS}\|} \quad (38)$$

$$\varepsilon_{geom} = \frac{\|\mathbf{p}^{Iter} - \mathbf{p}^{Real}\|}{\|\mathbf{p}^{Real}\|} \quad (39)$$

We also study the behavior of the algorithm on different regularization matrices. For this purpose, we propose five regularization matrices as linear combinations of \mathbf{L}_0 , \mathbf{L}_1 , \mathbf{L}_2 (Eq. 20) and solve the inverse geometry problem for each case.

The aim of these studies is to determine the optimal regularization matrix analyzing the stability of the algorithm against measurements with different levels of noise, and validate the algorithm developed as a reliable tool for estimating the location of the 1150°C isotherm in a blast furnace hearth.

In Tables 3, 4, 5 and 6, we show the relative errors ε_{obs} and ε_{geom} , and the number of iterations required to solve the problem, for each set of weighting factors (w_0, w_1, w_2) and for each noise level.

Analyzing these results we conclude that:

- As is expected, the relative error ε_{obs} increases as the *noise* increases.
- The algorithm is equally stable for different regularization matrices when measurements have a low level of noise because ε_{geom} remains stable in all cases (Table 4).
- The optimal regularization matrix appears to be (0.00, 0.00, 1.00) because the solutions have the lowest errors on the estimated geometry, ε_{geom} , particularly when measurements have a high level of noise (Tables 5 and 6).
- Even though 15% is a high level of noise, the geometry is estimated with good accuracy in the context of the industrial application (Fig. 6).

Finally, we can conclude that the algorithm developed is a reliable tool for estimating the location of the 1150°C isotherm in a blast furnace hearth.

6 CONCLUSIONS

We have developed a inverse geometry model for estimating the location of the 1150°C isotherm in a blast furnace hearth. The observations of the inverse problem are temperature measurements at points inside the object and the unknown is the geometry of the volume where the problem is defined. Due to the instability of ill-posed problems and the nonlinearity of our inverse problem, we have used the iteratively regularized Gauss-Newton method.

Case	w_0	w_1	w_2	ε_{geom} [%]	ε_{obs} [%]	Iter
1	1.00	0.00	0.00	1.283	0.354	6
2	0.00	1.00	0.00	1.798	0.872	5
3	0.00	0.00	1.00	0.582	0.376	5
4	0.00	0.50	0.50	0.646	0.284	5
5	0.50	0.50	0.00	0.408	0.247	6

Table 3: $noise = 0\%$ and $\mathbf{p}^\Delta = (1.000, 1.000, 1.000, 0.850, 0.750, 0.700, 0.700)^T$.

Case	w_0	w_1	w_2	ε_{geom} [%]	ε_{obs} [%]	Iter
1	1.00	0.00	0.00	2.457	2.127	5
2	0.00	1.00	0.00	2.774	2.119	6
3	0.00	0.00	1.00	2.560	2.136	5
4	0.00	0.50	0.50	2.628	2.129	5
5	0.50	0.50	0.00	2.855	2.122	5

Table 4: $noise = 5\%$ and $\mathbf{p}^\Delta = (1.000, 1.000, 1.000, 0.850, 0.750, 0.700, 0.700)^T$.

Case	w_0	w_1	w_2	ε_{geom} [%]	ε_{obs} [%]	Iter
1	1.00	0.00	0.00	12.284	4.163	6
2	0.00	1.00	0.00	11.241	4.171	5
3	0.00	0.00	1.00	6.647	4.632	4
4	0.00	0.50	0.50	8.025	4.446	4
5	0.50	0.50	0.00	12.411	4.123	6

Table 5: $noise = 10\%$ and $\mathbf{p}^\Delta = (1.000, 1.000, 1.000, 0.850, 0.750, 0.700, 0.700)^T$.

Case	w_0	w_1	w_2	ε_{geom} [%]	ε_{obs} [%]	Iter
1	1.00	0.00	0.00	11.175	4.900	8
2	0.00	1.00	0.00	11.964	4.853	5
3	0.00	0.00	1.00	9.974	5.426	7
4	0.00	0.50	0.50	10.172	5.070	6
5	0.50	0.50	0.00	11.108	4.885	6

Table 6: $noise = 15\%$ and $\mathbf{p}^\Delta = (1.000, 1.000, 1.000, 0.850, 0.750, 0.700, 0.700)^T$.

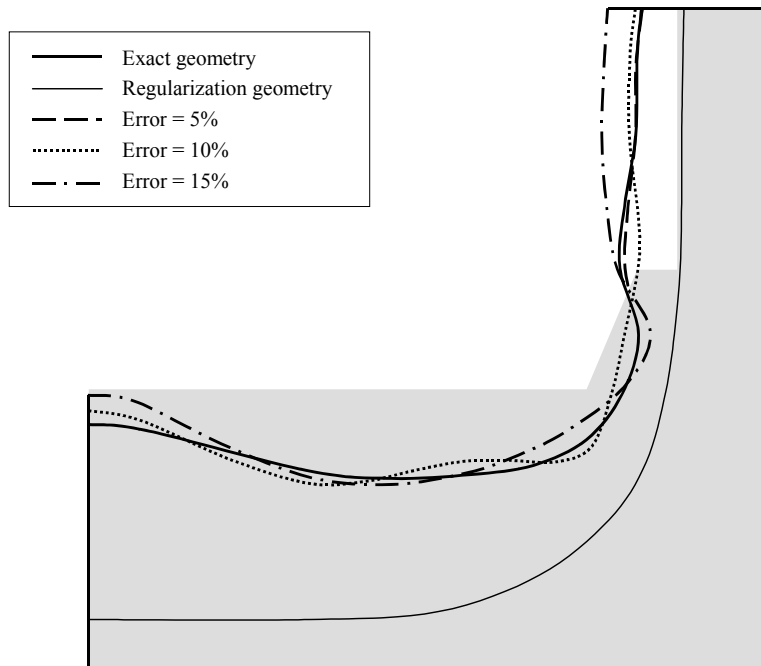


Figure 6: Estimated geometry for different levels of noise.

The location of the unknown boundary has been parametrized by a set of parameters and described with radial basis functions because they impose few restrictions on the geometry and provide a smooth interpolation.

The behavior of the algorithm on different regularization matrices has been studied analyzing its stability against simulated measurements with different levels of noise.

We can conclude, from the results of the analyzed cases, that the optimal regularization matrix appears to be L_2 , the discrete approximation of the second derivative operator, and that the geometry is estimated with good accuracy in the context of the industrial application.

To sum up, we conclude that the algorithm developed is a reliable tool for estimating the location of the 1150°C isotherm in a blast furnace hearth.

REFERENCES

- [1] Torrkulla J and Saxén H, “Model of the state of the blast furnace hearth”, *ISIJ International* 2000; **40**(5):438-447.
- [2] Sorli K and Skaar IM, “Monitoring the wear-line of a melting furnace”. *3rd Int. Conference on Inverse Problems in Engineering* 1999, Port Ludlow, WA, 1999.
- [3] Schulte M, Klima R, Ringel D, Voss M, “Improved wear-control at the blast furnace hearth by direct heat-flux measurements”. *Ironmaking Conference Proceedings* 1998; 607-614.
- [4] Kurpisz K, “A method for determining steady state temperature distribution within blast furnace hearth lining by measuring temperature at selected points”. *Transactions ISIJ*

- 1988; 28:926-929.
- [5] Gonzalez M, Goldschmit MB, Zubimendi JL, Gonzalez N, Ametrano R, Giandomenico F. "Inverse geometry problem of estimating the location of the 1150°C isotherm in a blast furnace hearth". *4th IAS Ironmaking Conference*. San Nicolás, Argentina, 2003; 381-386.
 - [6] Engl HW, Hanke M, Neubauer A. *Regularization of inverse problems*. Kluwer Academic Publishers, 1996.
 - [7] Alifanov OM. *Inverse heat transfer problems*. Springer-Verlag, 1994.
 - [8] Kaltenbacher B. "On convergence rates of some iterative regularization methods for an inverse problem for nonlinear parabolic equation connected with continuous casting of steel". *J. Inv. Ill-Posed Problems* 1999; 7(2):145-164.
 - [9] Jin QN. "The analysis of a discrete scheme of the iteratively regularized Gauss-Newton method". *Inverse Problems* 2000; 16:1457-1476.
 - [10] Kaltenbacher B, Neubauer A, Ramm AG. "Convergence rates of the continuous regularized Gauss-Newton method". *J. Inv. Ill-Posed Problems* 2002; 10(3):261-280.
 - [11] Doicu A, Schreier F, Hess M, "Iteratively regularized Gauss-Newton method for atmospheric remote sensing". *Computer Physics Communications* 2002; 148:214-226.
 - [12] Carr JC, Beatson RK, Cherrie JB, Mitchell TJ, Fright WR, McCallum BC. "Reconstruction and representation of 3D objects with radial basis functions". *ACM SIGGRAPH 2001*. Los Angeles, CA, 2001; 67-76.
 - [13] Carr JC, Fright TJ, Batson RK. "Surface interpolation with radial basis functions for medical imaging". *IEEE Transactions on Medical Imaging* 1997; 20(Y):1-18.
 - [14] Perrin F, Bertrand O, Pernier J. "Scalp current density mapping: value and estimation from potential data". *IEEE Transactions on Biomedical Engineering* 1987; BME-34(4):283-288.
 - [15] Belytschko T, Parimi C, Moes N, Sukumar N, Usui S. "Structured extended finite element method for solids defined by implicit surfaces". *Int. J. Numer. Meth. Engng* 2003; 56:609-635.
 - [16] Bathe KJ. *Finite element procedures*. Prentice-Hall, 1996.
 - [17] Zienkiewicz OC, Taylor RL. *The Finite Element Method* (4th edn). McGraw-Hill: New York, 1989.
 - [18] Appel JR and Gunzburger MD. "Sensitivity calculation in flows with discontinuities". *Proc. 14th AIAA Applied Aerodynamics Conference* New Orleans, USA 1996.
 - [19] Brezinski C, Redivo-Zaglia M, Rodriguez G, Seatzu S. "Multi-parameter regularization techniques for ill-conditioned linear systems". *Numer. Math.* 2003. 94:203-228.